# High Time Resolution Electron Paramagnetic Resonance of Light-Induced Radical Pairs in Photosynthetic Bacterial Reaction Centers: Observation of Quantum Beats

**Gerd Kothe,*,‡ Stefan Weber,‡ Ernst Ohmes,‡ Marion C. Thurnauer,† and James R. Norris†**

*Contribution from the Department of Physical Chemistry, University of Stuttgart, Pfaffenwaldring 55, D-70569 Stuttgart, Germany, and Chemistry Division, Argonne National Laboratory, Argonne, Illinois 60439*

*Received September 23, 1993**

**Abstract:** Light-induced radical pairs in fully deuterated photosynthetic reaction centers of purple bacteria *Rhodobacter sphaeroides* have been studied by high time resolution electron paramagnetic resonance. *Quantum beat oscillations* are detected at early times after laser excitation for native and iron-removed reaction center preparations. Due to their spin-correlated generation, the secondary radical pairs $P^+[QFe^{2+}]^-$ and $P^+Q^-$ are expected to start out in a coherent superposition of eigenstates, as observed experimentally. Analysis of the *quantum beats* as a function of the static magnetic field can ultimately provide detailed information on the molecular structure of the short-lived intermediates in the primary steps of bacterial photosynthesis.

## Introduction

Spin-correlated radical pairs (rps)[1-6] are generated as short-lived intermediates in the primary energy conversion steps of natural and artificial photosynthesis.[1,4-15] If the initial configuration of the rp (singlet or triplet) is not an eigenstate of the corresponding spin Hamiltonian, the rp starts out in a coherent superposition of two of the four spin states,[16-19] which can manifest itself as *quantum beats* in an electron paramagnetic resonance (EPR) experiment with adequate time resolution.[20,21] In the following we report observation of *quantum beats* for the light-induced rps in purple photosynthetic bacterial reaction center proteins (rcs) and suggest how they may be used to obtain new structural details of the rc.

In the photosystem of purple bacteria *Rhodobacter sphaeroides* the initial steps are[22,23]

$$PHQFe^{2+} \xrightarrow{h\nu} {}^1P^*HQFe^{2+} \xrightarrow{\sim 2.8\ ps} P^+H^-QFe^{2+} \xrightarrow{\sim 200\ ps} P^+H[QFe^{2+}]^- \quad (T < 50\ K) \quad (1)$$

where P is a special pair of bacteriochlorophylls, H is bacteriopheophytin, and Q is ubiquinone, which (in its reduced form) interacts with high-spin $Fe^{2+}$. As a result, light-induced polarized EPR signals from native bacterial rcs are not observed except at cryogenic temperatures,[14,24,25] where the $[QFe^{2+}]^-$ complex can be modeled by two doublets, characterized by a large **g**-tensor anisotropy.[26-28] We report high time resolution transient EPR of fully deuterated (99.7%) iron-removed rcs of *Rb. sphaeroides* R26, and discuss the results together with those from native preparations.

## Experimental Section

**Sample Preparation.** Deuterated rcs were isolated from whole cells of *Rb. sphaeroides* R26 which were grown in $D_2O$ (99.7%) on deuterated substrates.[29] Rcs were isolated according to the procedures described by

† Argonne National Laboratory.
‡ University of Stuttgart.

(1) Thurnauer, M. C.; Norris, J. R. *Chem. Phys. Lett.* **1980**, *76*, 557–561.
(2) Closs, G. L.; Forbes, M. D. E.; Norris, J. R. *J. Phys. Chem.* **1987**, *91*, 3592–3599.
(3) Buckley, C. D.; Hunter, D. A.; Hore, P. J.; MacLauchlan, K. H. *Chem. Phys. Lett.* **1987**, *135*, 307–312.
(4) Hore, P. J.; Hunter, D. A.; McKie, C. D.; Hoff, A. J. *Chem. Phys. Lett.* **1987**, *137*, 495–500.
(5) Stehlik, D.; Bock, C. H.; Petersen, J. *J. Phys. Chem.* **1989**, *93*, 1612–1619.
(6) Hore, P. J. In *Advanced EPR, Applications in Biology and Biochemistry*; Hoff, A. J., Ed.; Elsevier: Amsterdam, 1989; pp 405–440.
(7) Stehlik, D.; Bock, C. H.; Thurnauer, M. C. In *Advanced EPR, Applications in Biology and Biochemistry*; Hoff, A. J., Ed.; Elsevier: Amsterdam, 1989; pp 371–403.
(8) Feezel, L. L.; Gast, P.; Smith, U. H.; Thurnauer, M. C. *Biochim. Biophys. Acta* **1989**, *974*, 149–155.
(9) Hasharoni, K.; Levanon, H.; Tang, J.; Bowman, M. K.; Norris, J. R.; Gust, D.; Moore, T. A.; Moore, A. L. *J. Am. Chem. Soc.* **1990**, *112*, 6477–6481.
(10) Morris, A. L.; Norris, J. R.; Thurnauer, M. C. In *Reaction Centers of Photosynthetic Bacteria*; Michel-Beyerle, M.-E., Ed.; Springer Series in Biophysics, Springer-Verlag: Berlin, 1990; Vol. 6, pp 423–435.
(11) Wasielewski, M. R.; Gaines, G. L.; O'Neil, M. P.; Svec, W. A.; Niemczyk, M. P. *J. Am. Chem. Soc.* **1990**, *112*, 4559–4560.
(12) Norris, J. R.; Morris, A. L.; Thurnauer, M. C.; Tang, J. *J. Chem. Phys.* **1990**, *92*, 4239–4249.
(13) Schlüpmann, K. M.; Salikhov, K. M.; Plato, M.; Jaegermann, P.; Lendzian, F.; Möbius, K. *Appl. Magn. Reson.* **1991**, *2*, 117–142.
(14) Snyder, S. W.; Morris, A. L.; Bondeson, S. R.; Norris, J. R.; Thurnauer, M. C. *J. Am. Chem. Soc.* **1993**, *115*, 3774–3775.
(15) Snyder, S.; Thurnauer, M. C. In *The Photosynthetic Reaction Center*; Deisenhofer, J., Norris, J. R., Eds.; Academic Press, Inc.: New York, 1993; pp 285–330.
(16) Salikhov, K. M.; Bock, C. H.; Stehlik, D. *J. Appl. Magn. Reson.* **1990**, *1*, 195–211.
(17) Bittl, R.; Kothe, G. *Chem. Phys. Lett.* **1991**, *177*, 547–553.
(18) Wang, Z.; Tang, J.; Norris, J. R. *Magn. Reson.* **1992**, *97*, 322–334.
(19) Zwanenburg, G.; Hore, P. J. *Chem. Phys. Lett.* **1993**, *203*, 65–74.
(20) Kothe, G.; Weber, S.; Bittl, R.; Norris, J. R.; Snyder, S. S.; Tang, J.; Thurnauer, M. C.; Morris, A. L.; Rustandi, R. R.; Wang, Z. In *Spin Chemistry*; I'Haya, Y. J., Ed.; The Oji International Conference on Spin Chemistry: Tokyo, 1991; pp 420–434.
(21) Kothe, G.; Weber, S.; Bittl, R.; Ohmes, E.; Thurnauer, M. C.; Norris, J. R. *Chem. Phys. Lett.* **1991**, *186*, 474–480.
(22) Kirmaier, C.; Holton, D.; Parson, W. W. *Biochim. Biophys. Acta* **1985**, *810*, 33–48.
(23) *The Photosynthetic Reaction Center*; Deisenhofer, J., Norris, J. R., Eds.; Academic Press: New York, 1993.
(24) Proskuryakov, I. I.; Shkuropatov, A. Ya.; Sarrazian, N. A.; Shuvalov, V. A. *Dokl. Akad. Nauk SSSR* (Russian) **1991**, *320*, 1006–1008.
(25) Proskuryakov, I. I.; Klenina, I. B.; Shkuropatov, A. Ya.; Shkuropatova, V. A.; Shuvalov, V. A. *Biochim. Biophys. Acta* **1993**, *1142*, 207–210.
(26) Butler, W. F.; Johnston, D. C.; Shore, H. B.; Fredkin, D. R.; Okamura, M. Y.; Feher, G. *Biophys. J.* **1980**, *32*, 967–992.
(27) Calvo, R.; Butler, W. F.; Isaacson, R. A.; Okamura, M. Y.; Fredkin, D. R.; Feher, G. *Biophys. J.* **1982**, *37*, 111a.
(28) Butler, W. F.; Calvo, R.; Fredkin, D. R.; Isaacson, R. A.; Okamura, M. Y.; Feher, G. *Biophys. J.* **1984**, *45*, 947–973.
(29) Crespi, H. L. In *Methods in Enzymology*; Packer, L., Ed.; Academic Press: New York, 1982; Vol. 88, pp 3–5.

0002-7863/94/1516-7729$04.50/0 

Wraight.[30] The method by Tiede and Dutton[31] was followed for removal of $Fe^{2+}$ from the rcs. Samples for the EPR experiments were prepared by filling the rc solutions (deuterated tricine buffer) into a quartz tube (2-mm inner diameter) located in the symmetry axis of the microwave resonator. The temperature of the samples was controlled using a helium flow cryostat (Oxford CF:935) and was stable to ±0.1 K.

**EPR Measurements.** The basic concept of the EPR experiment is similar to that described previously.[21,32] A modified X-band spectrometer (Bruker ER-200 D) was used, equipped with a fast microwave preamplifier (36 dB, 1.8 dB noise figure) and a broad band video amplifier (band width 200 Hz–200 MHz). The sample was irradiated in a home-built split ring resonator with 2 ns pulses of an Nd:YAG pumped dye laser (Spectra Physics, 580 nm, 10 mJ/pulse) at a repetition rate of 10 Hz. The split ring resonator exhibits a high filling factor at low $Q$ (unloaded $Q \approx 500$) and provides an easy means of sample irradiation.

The time-dependent EPR signal was digitized in a transient recorder (LeCroy 9450 digital oscilloscope) at a rate of 2.5 ns/12 bit sample. The time resolution of the experimental setup is estimated to be in the 10-ns range. Typically, 512 transients were accumulated at off-resonance conditions and subtracted from those on resonance to get rid of the laser background signal. As demonstrated shortly, the best overall view of the full data set is obtained from a two-dimensional plot of the signal intensity versus the time and magnetic field axis.

## Theoretical Background

In this section we briefly summarize a model for transient EPR of spin-correlated rps and define the model parameters.[17,21,33] Specifically, we consider a sudden, light-induced generation of the rp with a spatially fixed geometry. Particular emphasis is given to the slow-motional regime where anisotropic magnetic interactions dominate.

**Spin Hamiltonian.** The total spin Hamiltonian, $\mathcal{H}(\Omega,t)$, depends on the orientation, $\Omega$, of the rp and can be divided in five parts

$$\mathcal{H}(\Omega,t) = \mathcal{H}_Z(\Omega) + \mathcal{H}_R(\Omega,t) + \mathcal{H}_{EX} + \mathcal{H}_D(\Omega) + \mathcal{H}_{HF}(\Omega) \tag{2}$$

The first term, describing Zeeman interactions of the electron spins $\mathbf{S}_i$, $i = 1,2$, with the static magnetic field $\mathbf{B}_0 = (0,0,B_0)$ is given by

$$\mathcal{H}_Z(\Omega) = \beta\mathbf{B}_0\cdot[\mathbf{g}_1(\Omega)\cdot\mathbf{S}_1 + \mathbf{g}_2(\Omega)\cdot\mathbf{S}_2] \tag{3}$$

where $\beta$ and $\mathbf{g}_i$, $i = 1,2$, are the Bohr magneton and the g-tensor of radical $i$, respectively.

In the presence of a rotating microwave field $\mathbf{B}_1 = (B_1 \cos \omega t, B_1 \sin \omega t, 0)$ the Hamiltonian includes the radiation term

$$\mathcal{H}_R(\Omega,t) = \beta\mathbf{B}_1\cdot[\mathbf{g}_1(\Omega)\cdot\mathbf{S}_1 + \mathbf{g}_2(\Omega)\cdot\mathbf{S}_2] \tag{4}$$

where $B_1$ denotes the magnitude of the microwave radiation. The next two terms of eq 2 account for the isotropic and anisotropic spin–spin coupling of the rp

$$\mathcal{H}_{EX} = J(Q_T - Q_S) \tag{5}$$

$$\mathcal{H}_D(\Omega) = (\mathbf{S}_1 + \mathbf{S}_2)\cdot\mathbf{D}(\Omega)\cdot(\mathbf{S}_1 + \mathbf{S}_2) \tag{6}$$

$$Q_T = \left(\frac{3}{4} + \mathbf{S}_1\cdot\mathbf{S}_2\right) \tag{7}$$

$$Q_S = \left(\frac{1}{4} - \mathbf{S}_1\cdot\mathbf{S}_2\right) \tag{8}$$

where $J$, $\mathbf{D}(\Omega)$ are the electron exchange interaction and dipolar coupling tensor, respectively. Since $\mathbf{D}$ is traceless, two parameters, $D$ and $E$, completely determine this tensor.

The last term of the Hamiltonian 2 describes the magnetic interactions between electron and nuclear spins. For weakly coupled rps this part of the Hamiltonian can be written as[34]

$$\mathcal{H}_{HF}(\Omega) = \sum_k \mathbf{I}_{1k}\cdot\mathbf{A}_{1k}(\Omega)\cdot\mathbf{S}_1 + \sum_l \mathbf{I}_{2l}\cdot\mathbf{A}_{2l}(\Omega)\cdot\mathbf{S}_2 \tag{9}$$

where $\mathbf{I}_{ik}$ is the spin operator of nucleus $k$ in radical $i$ and $\mathbf{A}_{ik}(\Omega)$ is the corresponding hyperfine tensor. $a_{ik}$ denotes the isotropic hyperfine coupling constant

$$a_{ik} = \frac{1}{3}(A_{ik}^X + A_{ik}^Y + A_{ik}^Z) \tag{10}$$

and $A_{ik}^j$, $j = X, Y, Z$, are the principal values of $\mathbf{A}_{ik}$, respectively.

Because of the explicit time dependence of $\mathcal{H}_R(\Omega,t)$ we transform into a frame of reference, rotating with the microwave frequency $\omega$ around the static magnetic field $\mathbf{B}_0$. This transformation is not a matter of pictorial convenience, but an essential step toward a proper theoretical analysis.[35] Neglect of all nonsecular terms, as usual in the high-field approximation, renders the transformed Hamiltonian $\mathcal{H}^r(\Omega)$ virtually time independent.

**Stochastic Liouville Equation.** Generally, the time evolution of the density matrix, $\rho^r(t)$, is described by the stochastic Liouville equation[36,37]

$$\frac{\partial}{\partial t}\rho^r(\Omega,t) = -i[(1/\hbar)\mathbf{H}^{xr}(\Omega) - i\mathbf{L}(\Omega) + i\mathbf{R}]\cdot\rho^r(\Omega,t) \tag{11}$$

which we solve using a finite grid point method.[38,39] Here $\mathbf{H}^{xr}(\Omega)$ denotes a superoperator associated with the spin Hamiltonian $\mathcal{H}^r(\Omega)$ of the rp. $\mathbf{L}(\Omega)$ is the stationary Markov operator for the various rotational processses, and $\mathbf{R}$ is a phenomenological relaxation superoperator.

The specific form of the Markov operator $\mathbf{L}(\Omega)$ depends on the model used to describe the motions.[32] For isotropic tumbling of the rp as the only motional process, $\mathbf{L}(\Omega)$ can be expressed in terms of a single rotational correlation time $\tau_R$ and the equilibrium populations $\mathbf{P}_{eq}(\Omega)$ of the orientations. In the slow-motional limit ($\tau_R > 10^{-6}$ s), applying to the present case, $\mathbf{L}(\Omega)$ may be dropped. The relaxation superoperator $\mathbf{R}$ accounts for all relaxation processes neglected in truncating $\mathbf{H}^{xr}(\Omega)$ and $\mathbf{L}(\Omega)$. Generally, the elements of $\mathbf{R}$ can be related to the residual relaxation times $T_1$ and $T_2$ as described elsewhere.[17,33]

Formally, integration of eq 11 leads to

$$\rho^r(\Omega,t) = \exp\{-[(i/\hbar)\mathbf{H}^{xr}(\Omega) + \mathbf{L}(\Omega) - \mathbf{R}]t\}\cdot\rho^r(\Omega,0) \tag{12}$$

where $\rho^r(\Omega,0)$ is the initial condition of the density matrix at the time of the sudden generation of the rp. Only in the case of primary rps do we expect pure initial spin states

$$\rho^r(\Omega,0) = \mathbf{P}_{eq}(\Omega)\cdot\mathbf{Q}_i; \qquad i = S, T \tag{13}$$

determined by the spin multiplicity of the excited precursor. For all following pairs, the pure singlet might be admixed with some triplet character and vice versa.[12,14] In these cases $\rho^r(\Omega,0)$ can be evaluated by solving eq 11 for the lifetime of the precursor rp.

(30) Wraight, C. A. *Biochim. Biophys. Acta* **1979**, *548*, 309–327.
(31) Tiede, D. M.; Dutton, P. L. *Biochim. Biophys. Acta* **1981**, *637*, 278–290.
(32) Münzenmaier, A.; Rösch, N.; Weber, S.; Feller, C.; Ohmes, E.; Kothe, G. *J. Phys. Chem.* **1992**, *96*, 10645–10653.
(33) Kothe, G.; Weber, S.; Ohmes, E.; Thurnauer, M. C.; Norris, J. R. *J. Phys. Chem.* **1994**, *98*, 2706–2712.
(34) Reitz, D. C.; Weissman, S. I. *J. Chem. Phys.* **1960**, *33*, 700–704.
(35) Redfield, A. G. *Phys. Rev.* **1955**, *98*, 1787–1801.
(36) Kubo, R. In *Fluctuation, Relaxation and Resonance in Magnetic Systems*; ter Haar, D., Ed.; Oliver and Boyd: Edinburgh, 1962; pp 23–68.
(37) Freed, J. H.; Bruno, G. V.; Polnaszek, C. F. *J. Phys. Chem.* **1971**, *75*, 3385–3399.

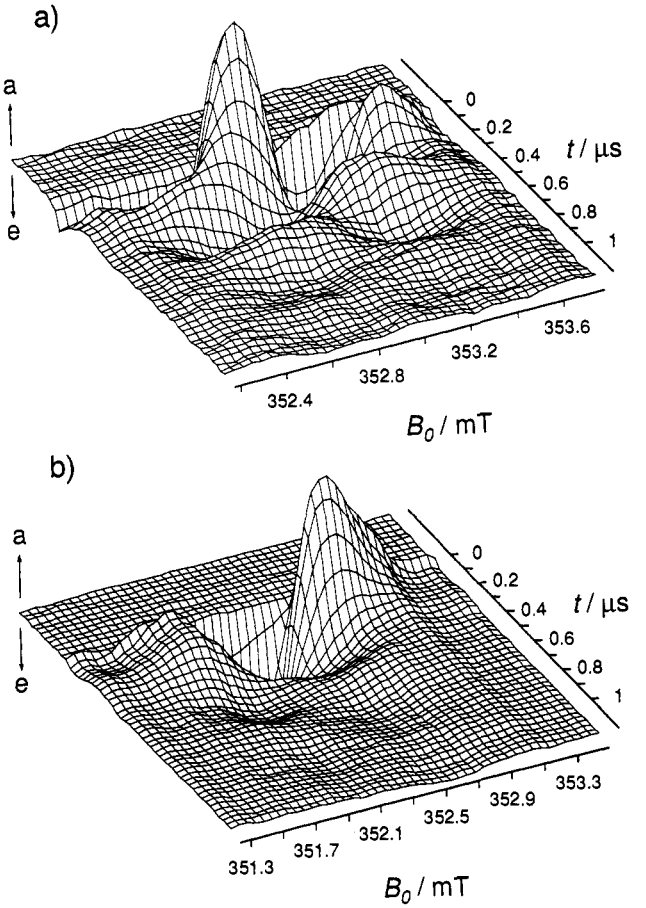


**Figure 1.** Complete data sets of the transient EPR signal of light-induced radical pairs in 99.7% deuterated bacterial reaction centers of *Rhodobacter sphaeroides* R26. Positive and negative signals indicate absorptive (a) and emissive (e) polarizations, respectively: microwave field, $B_1 = 0.08$ mT; temperature, $T = 10$ K. (a) Data set of secondary radical pairs $P^+Q^-$ in iron-removed reaction centers. Microwave frequency $\omega/2\pi = 9.8997$ GHz. (b) Data set of secondary radical pairs $P^+$ $[QFe^{2+}]^-$ in iron-containing reaction centers. Microwave frequency $\omega/2\pi = 9.8811$ GHz.

Evaluating the trace of $\rho^r(t)\cdot(S_1^y + S_2^y)$ finally gives the observable EPR signal of the transient nutation experiment as

$$M(t) = \mathrm{Tr}[\rho^r(t)\cdot(S_1^y + S_2^y)] \quad (14)$$

$$\rho^r(t) = \int \rho^r(\Omega,t)\,d\Omega \quad (15)$$

where $\rho^r(\Omega,t)$ is obtained by solving eq 12. The corresponding diagonalizations were accomplished using the Rutishauser algorithm according to Gordon and Messenger.[40] For this purpose, Fortran routines have been adapted from the literature[40,41] and modified.[17]

## Experimental Results

Fully deuterated native and iron-depleted bacterial rcs of *Rb. sphaeroides* R26 were irradiated with 2 ns pulses of an Nd:YAG pumped dye laser, and the time evolution of the transverse magnetization was monitored for various static magnetic fields. Typical results are shown in Figures 1–4. The observed time profiles vary drastically according to the experimental parameters employed.

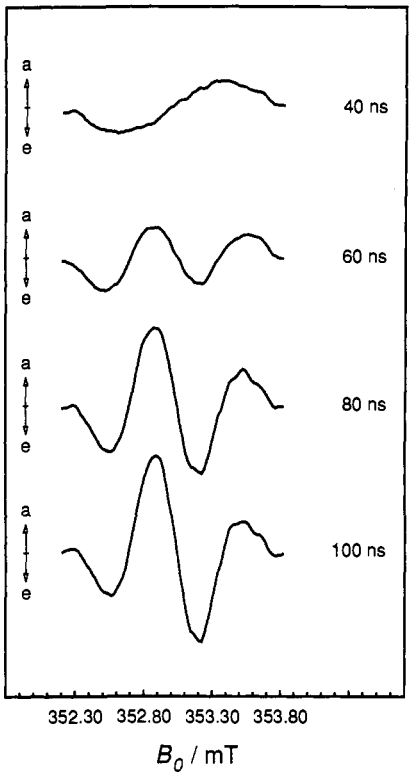


**Figure 2.** Transient EPR line shapes of the light-induced radical pairs $P^+Q^-$ in 99.7% deuterated iron-removed bacterial reaction centers of *Rhodobacter sphaeroides* R26 at various times after the laser pulse. Time window = 10 ns. Positive and negative signals indicate absorptive (a) and emissive (e) polarization, respectively: microwave frequency, $\omega/2\pi = 9.8997$ GHz; microwave field, $B_1 = 0.08$ mT; temperature, $T = 10$ K.

**Complete Data Sets.** As described in the Experimental Results, a complete data set consists of transient signals taken at equidistant magnetic field points covering the total spectral width. This implies a two-dimensional variation of the signal intensity with respect to both the magnetic field and time axis. Such a complete data set can be conveniently presented in a two-dimensional plot as shown in Figure 1 for iron-removed (a) and iron-containing (b) rcs. The plots refer to a constant microwave magnetic field of $B_1 = 0.08$ mT and $T = 10$ K. Note that a positive signal indicates absorptive (a) and a negative emissive (e) spin polarization.

Transient spectra can be extracted from this plot at any fixed time after the laser pulse as slices parallel the magnetic field axis. Likewise, the time evolution of the transverse magnetization may be obtained for any given field as a slice along the time axis. In the following, transient spectra and time profiles are presented separately.

**Transient Spectra.** Typical line shapes for iron-depleted rcs, observed 40, 60, 80, and 100 ns after the laser pulse, are shown in Figure 2. They refer to a microwave field of $B_1 = 0.08$ mT and $T = 10$ K. Each spectrum is integrated over a narrow time window of 10 ns. Apparently, the early spectrum is much broader than the later ones. Moreover, the polarization changes from a simple e/a pattern at early times to a characteristic e/a/e/a pattern at later times. A detailed analysis reveals that lifetime broadening actually dominates the early spectrum.[33]

Figure 3 compares stationary spectra for iron-removed (a) and iron-containing (b) rcs, averaged in the time gate 400–440 ns after laser excitation. The spectra refer to $T = 10$ K. In order to avoid line shape distortions by Torrey oscillations a reduced microwave field of $B_1 = 0.01$ mT has been employed.

The e/a/e/a pattern for the iron-removed sample was observed over the entire long time range of our experiments. Evidence for a triplet spectrum of the primary donor P was not obtained. Even though we have not measured the lifetime of $P^+H^-$ independently, the absence of triplet signal indicates that this intermediate is short-lived.[42-44] The results are

(38) Norris, J. R.; Weissman, S. I. *J. Phys. Chem.* **1969**, *73*, 3119–3124.
(39) Kothe, G. *Mol. Phys.* **1977**, *33*, 147–158.
(40) Gordon, R. G.; Messenger, T. In *Electron Spin Relaxation in Liquids*; Muus, L. T., Atkins, P. W., Eds.; Plenum Press: New York, 1972; pp 341–381.
(41) Cullum, J.; Willoughby, R. A. *Lanczos Algorithmus for Large Symmetric Eigenvalue Computations*; Birkhäuser: Basel, 1985; Vol. 2.
(42) Liu, B.-L.; van Kan, P. J. M.; Hoff, A. J. *FEBS Lett.* **1991**, *289*, 23–28.
(43) Schelvis, J. P. M.; Liu, B.-L.; Aartsma, T. J.; Hoff, A. J. *Biochim. Biophys. Acta* **1992**, *1102*, 229–236.

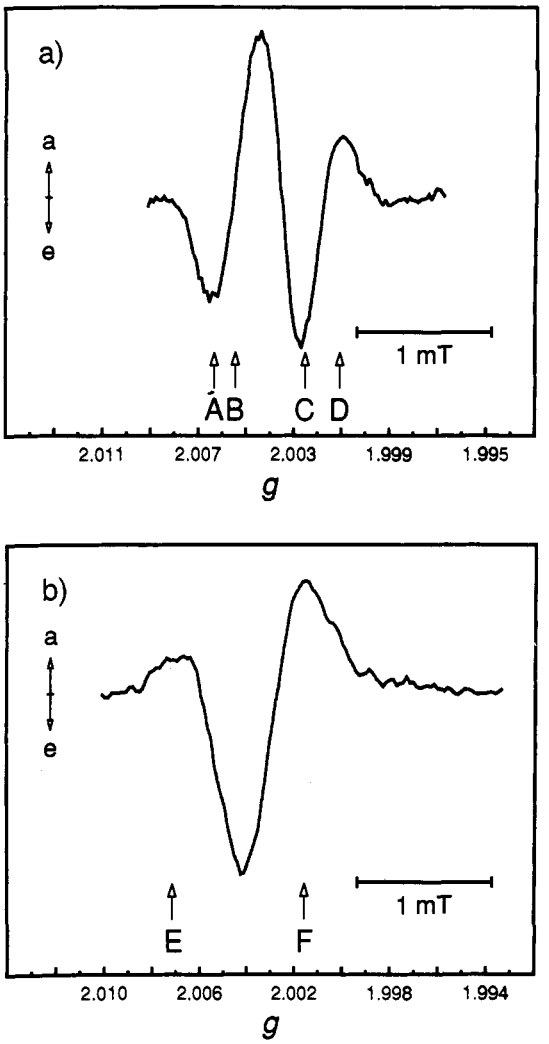


**Figure 3.** Stationary EPR spectra of light-induced radical pairs in 99.7% deuterated bacterial reaction centers of *Rhodobacter sphaeroides* R26. Spectra were taken 400–440 ns after laser excitation. Positive and negative signals indicate absorptive (a) and emissive (e) polarizations, respectively: microwave field, $B_1$ = 0.01 mT; temperature, $T$ = 10 K. (a) Spectrum of secondary radical pairs $P^+Q^-$ in iron-removed reaction centers. Microwave frequency, $\omega/2\pi$ = 9.8997 GHz. (b) Spectrum of secondary radical pairs $P^+[QFe^{2+}]^-$ in iron-containing reaction centers. Microwave frequency, $\omega/2\pi$ = 9.8811 GHz.

in agreement with those made on similar preparations under comparable conditions.[8,15] Therefore, the e/a/e/a pattern can be assigned to the secondary rp $P^+Q^-$. Model calculations,[17,21,33] based on the spin-correlated rp concept,[1-6] indicate the anisotropic nature[4,6,15] of this spectrum. However, the spectral resolution, even for a fully deuterated sample, is not sufficient to evaluate the various parameters unambiguously.

The stationary spectrum for iron-containing rcs is presented in Figure 3b. The experimental conditions were the same as those used for the iron-removed sample ($B_1$ = 0.01 mT, $T$ = 10 K). Yet, the observed polarization differs significantly, starting absorptive at the low-field end. The distinct a/e/a pattern, centered at $g$ = 2.0026, corresponds to previous observations.[14,24,25]

**Time Profiles.** Figure 4 (left column) depicts the time evolution of the transverse magnetization for iron-removed rcs, measured with a resolution of 10 ns.[21,33] The transients refer to a constant microwave field of $B_1$ = 0.08 mT, $T$ = 10 K, and four selected field positions (A–D, Figure 3a). Apparently, all transients exhibit oscillatory behavior at early times after the laser pulse. Note, however, that the frequency of these oscillations varies across the spectrum, indicating an anisotropic nature of the transients.

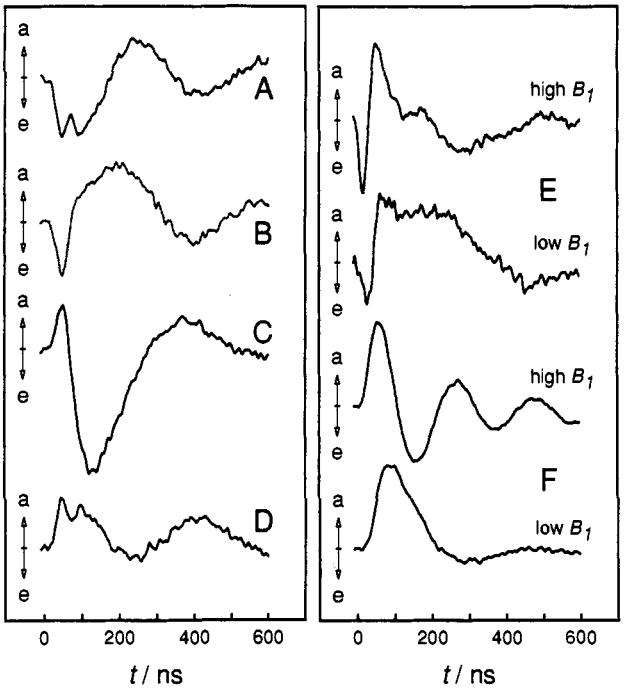


**Figure 4.** Time evolution of the transverse magnetization of light-induced radical pairs in 99.7% deuterated bacterial reaction centers of *Rhodobacter sphaeroides* R26. Time profiles were taken at various static magnetic fields (positions A–F, Figure 3). Positive and negative signals indicate absorptive (a) and emissive (e) polarizations, respectively: temperature, $T$ = 10 K. Left column: Experimental time profiles for the secondary radical pairs $P^+Q^-$ in iron-removed reaction centers. Microwave frequency, $\omega/2\pi$ = 9.8997 GHz. Microwave field, $B_1$ = 0.08 mT. Right column: Experimental time profiles for the secondary radical pairs $P^+[QFe^{2+}]^-$ in iron-containing reaction centers at two different microwave fields. $B_1$ = 0.15 mT (upper curves) and $B_1$ = 0.08 mT (lower curves). Microwave frequency, $\omega/2\pi$ = 9.8811 GHz.

Generally, oscillation frequencies of 10–20 MHz can be extracted from the profiles. In addition, isotropic Torrey oscillations[7,33] with a frequency of $\omega_1/2\pi \approx 2.2$ MHz can be seen. Basically, the fast oscillations represent *quantum beats* detected in the transverse magnetization. Observation of such coherence phenomena for deuterated samples of photosystem I from cyanobacteria has been reported recently.[20,21,33] Due to their spin-correlated generation, the secondary rps $P^+Q^-$ are expected to start out in a coherent superposition of eigenstates,[16-19] as observed experimentally. Detection of *quantum beats* in bacterial rcs confirms previous interpretations of the transient EPR spectrum employing the correlated rp concept.[4,6] Furthermore, the frequency of the beats and the amplitude variation ultimately provides a direct measurement of a number of important magnetic and structural parameters.[33]

Figure 4 (right column) depicts the time evolution of the transverse magnetization for native iron-containing rcs, measured at $T$ = 10 K. The transients were taken at two selected field positions (E and F, Figure 3b) and two different microwave magnetic fields ($B_1$ = 0.15 mT upper curves; $B_1$ = 0.08 mT lower curves). In all cases, slow oscillations with frequencies between two and four MHz are present. Closer inspection reveals that these oscillations not only result from Torrey precessions but also have components from nuclear coherences, generated by the nonadiabatic change of the spin Hamiltonian at the instant of the laser pulse.[45] In addition, at the low-field absorptive maximum (E, Figure 3b) fast initial oscillations with a frequency of 20 MHz are observed. As noted above, such oscillations may be assigned to *quantum beats* associated with the spin-correlated generation of a rp.

## Analysis of Experiments

**Parameter Values.** Analysis of the transient EPR experiments was performed employing the model outlined in the Theory section. Table 1 summarizes the parameters used in the calculations. The

(44) Gunner, M. R.; Robertson, D. E.; LoBrutto, R. L.; Mc.Laughlin, A. C.; Dutton, P. L. In *Progress in Photosynthetic Research*; Biggins, J., Ed.; M. Nijhoff: Dordrecht, 1987; Vol. I, pp 217–220.

(45) Weber, S.; Ohmes, E.; Thurnauer, M. C.; Norris, J. R.; Kothe, G., manuscript in preparation.

**Table 1.** Parameters Used in EPR Model Calculations for the Light-Induced Radical Pairs $P^+Q^-$ and $P^+[QFe^{2+}]^-$ in Iron-Removed and Native Bacterial Reaction Centers of *Rhodobacter Sphaeroides* R26

| g-tensors[a] | | | | | geometry[c] | |
|---|---|---|---|---|---|---|
| $P^+$ | $Q^-$ | $[QFe^{2+}]^-$ ground doublet | $[QFe^{2+}]^-$ first exc doubl | spin–spin coupling[b] | $P^+$ | dipol tensor |
| $g_P^X$, 2.0033 | $g_Q^X$, 2.0066 | $g_{QFe}^X$, 1.77 | $g_{QFe}^X$, 1.81 | $J$, 0 | $\phi_P$, −17° | $\phi_D$, arbitr |
| $g_P^Y$, 2.0025 | $g_Q^Y$, 2.0054 | $g_{QFe}^Y$, 0.60 | $g_{QFe}^Y$, 5.5 | $D$, −0.125 mT | $\theta_P$, 56° | $\theta_D$, 65° |
| $g_P^Z$, 2.0021 | $g_Q^Z$, 2.0022 | $g_{QFe}^Z$, 1.84 | $g_{QFe}^Z$, 1.71 | $E$, 0 | $\psi_P$, −2° | $\psi_D$, 59° |

[a] Data for $P^+$ and $Q^-$ from recent W-band EPR studies.[46,47] Analysis of the $[QFe^{2+}]^-$ complex revealed that the low temperature EPR spectrum can be modeled by two doublets, each characterized by a large g-tensor anisotropy.[28] [b] Estimated on the basis of the crystal structure of the reaction center complex.[48–50] [c] The Euler angles relate the principal axis system of the respective magnetic tensor and the molecular reference system (g-tensor of $Q^-$). Data from a transient K-band EPR study of zinc-substituted bacterial reaction centers.[51]

g-tensor components of $P^+$ and $Q^-$ were adopted from recent W-band EPR studies of *Rb. sphaeroides* rcs.[46,47] Magnetic characterization of the $[QFe^{2+}]^-$ complex in rcs from *Rb. sphaeroides* has previously been achieved.[26–28] Accordingly, the low temperature EPR spectrum of $[QFe^{2+}]^-$ can be modeled by two doublets, each characterized by a large g-tensor anisotropy.[28] The separation of the doublets is ~3 K.[28]

The spin–spin coupling parameters in the rps are estimates based on the crystal structure of the rc complex.[48–50] Angles for the magnetic tensor orientations in $P^+Q^-$ were adopted from a recent K-band EPR study of deuterated zinc-substituted rcs from *Rb. sphaeroides*.[51] The listed Euler angles relate the principal axis system of the respective magnetic tensor (g-tensor of $P^+$, dipolar coupling tensor) and the molecular reference system, collinear with the g-tensor of $Q^-$.[52] Data for the g-tensor orientations of the lowest doublets in $[QFe^{2+}]^-$ have been published recently.[53,54]

**Model Calculations.** Typically, 2000 grid points, regularly spaced over the surface of a sphere, were employed to simulate the static distribution of the rp with respect to the laboratory frame. In Figure 5 we compare experimental (left column) and calculated (right column) time profiles for $P^+Q^-$ in iron-removed bacterial rcs. The parameters for the calculations, intended to demonstrate the observation of *quantum beats*, are taken from the literature (see Table 1). Hyperfine interactions were approximated by considering four nitrogens ($a_N$ = 0.082 mT) in $P^+$ and four deuterons ($a_D$ = 0.076 mT) in $Q^-$, respectively. The residual relaxation times $T_1$ = 5 μs and $T_2$ = 800 ns have been estimated from the $B_1$ dependence of the effective decay of the transient magnetization. Inhomogeneous broadening was considered by convolution with a Gaussian of line width $\Delta B_0$ = 0.175 mT.

Generally, the agreement between observed and calculated transients is satisfactory. We thus conclude that the secondary rp $P^+Q^-$ is generated in a virtually pure singlet state, as assumed in the calculations. Notice that all transients start out with a horizontal slope. Then, amplitude and phase vary depending on the field position. Finally, 120 ns after the laser pulse all initial oscillations are averaged by residual hyperfine interactions in the fully deuterated sample.[33] This result shows that high time resolution is required for a successful EPR detection of *quantum beats*.

Preliminary model calculations for $P^+[QFe^{2+}]^-$, based on the published g-tensor parameters for the lowest doublets in $[QFe^{2+}]^-$,[28,53] (see Table 1) are in qualitative agreement with the experimental observations. We therefore conclude, that *quantum beat oscillations* have been detected in native iron-containing bacterial rcs. This result confirms the previous assignment of the transient spectrum (see Figure 3b) to $P^+$ from $P^+[QFe^{2+}]^-$.[14,25] Moreover, it explains why detection of *quantum beats* is restricted to only a few field positions. Because of the large g-tensor anisotropy associated with $[QFe^{2+}]^-$ the *beat frequencies* generally exceed our upper detection limit of ~100 MHz.

## Discussion

Light-induced rps in fully deuterated photosynthetic rcs of purple bacteria *Rb. sphaeroides* R26 have been studied by high time resolution transient EPR. *Quantum beat oscillations* are detected at early times after laser excitation for native and iron-removed rc preparations. In the following part we discuss how analysis of these coherence phenomena may provide insight into structure and function of the bacterial photosynthetic rc.

Under solid-state conditions the frequency of the *quantum beats*

$$\nu_{QB} = (1/h)\left\{\left[2J + \frac{2}{3}D^{zz}(\Omega)\right]^2 + [g_1^{zz}(\Omega) - g_2^{zz}(\Omega)]^2\beta^2B_0^2\right\}^{1/2} \quad (16)$$

critically depends on the orientation Ω of the rp in the laboratory frame ($z$ = direction of static magnetic field). The weak $B_1$ field, commonly employed in transient EPR, allows for only a small range of orientations to meet the resonance condition. Consequently, we expect the *beat frequencies* to vary significantly with $B_0$ across the powder spectrum, as observed experimentally (see Figure 4). The pronounced variation has been used to evaluate the geometry of the secondary rp in plant photosystem I.[33]

For zinc-substituted bacterial rcs the geometry of $P^+Q^-$ has recently been discussed.[51,55] The favored structure is based on the results of X-ray diffraction[48–50] and W-band EPR studies[46,47] of single crystal rcs proteins. In Figure 5 we compare experimental time profiles from iron-removed rcs (left column) with those calculated employing the favored geometry (right column).[51] Inspection reveals some deviations between experimental and calculated *beat frequencies*. These may be due to a number of factors, i.e., different sample conditions (zinc-substituted vs iron-removed preparations) or uncertainties in the employed geometry parameters. A simultaneous fit of several $B_0$ dependent time profiles could provide the necessary information.[33] Studies along these lines, involving different rc preparations,[43,44] are currently in progress.

(46) Klette, R.; Törring, J. T.; Plato, M.; Möbius, K.; Bönigk, B.; Lubitz, W. *J. Phys. Chem.* **1993**, *97*, 2015–2020.
(47) Burghaus, O.; Plato, M.; Rohrer, M.; Möbius, K.; McMillian, F.; Lubitz, W. *J. Phys. Chem.* **1993**, *97*, 7639–7647.
(48) Deisenhofer, J.; Epp, O.; Miki, K.; Huber, R.; Michel, H. *J. Mol. Biol.* **1984**, *180*, 385–398.
(49) Chang, C. H.; Tiede, D. M.; Tang, J.; Smith, U.; Norris, J. R.; Schiffer, M. *FEBS Lett.* **1986**, *205*, 82–86.
(50) Allen, J. P.; Feher, G.; Yeates, T. U.; Rees, D. C.; Deisenhofer, J.; Michel, H.; Huber, R. *Proc. Natl. Acad. Sci. U.S.A.* **1986**, *83*, 8589–8593.
(51) Van der Est, A.; Bittl, R.; Abresch, E. C.; Lubitz, W.; Stehlik, D. *Chem. Phys. Lett.* **1993**, *212*, 561–568.
(52) Hales, B. F. *J. Am. Chem. Soc.* **1975**, *97*, 5993–5997.
(53) Evelo, R. G.; Nan, H. M.; Hoff, A. J. *FEBS Lett.* **1988**, *239*, 351–357.
(54) Gast, P.; Gottschalk, A.; Norris, J. R.; Closs, G. L. *FEBS Lett.* **1989**, *243*, 1–4.
(55) Füchsle, G.; Bittl, R.; van der Est, A.; Lubitz, W.; Stehlik, D. *Biochim. Biophys. Acta* **1993**, *1142*, 23–35.

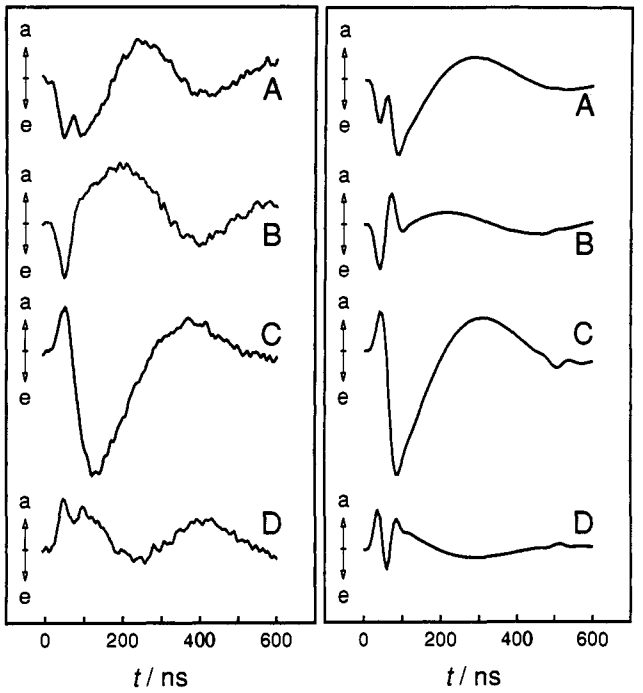


**Figure 5.** Time evolution of the transverse magnetization of the light-induced radical pairs $P^+Q^-$ in 99.7% deuterated bacterial reaction centers of *Rhodobacter sphaeroides* R26. Time profiles were taken at various static magnetic fields (position A–D, Figure 3a). Positive and negative signals indicate absorptive (a) and emissive (b) polarizations, respectively. Left column: Experimental time profiles at $T$ = 10 K. Microwave frequency, $\omega/2\pi$ = 9.8997 GHz. Microwave field, $B_1$ = 0.08 mT. Right column: Calculated time profiles using the parameters given in Table 1. Microwave frequency, $\omega/2\pi$ = 9.8997 GHz. Microwave field, $B_1$ = 0.08 mT. Inhomogeneous broadening, $\Delta B_0$ = 0.175 mT. Residual relaxation times $T_1$ = 5 $\mu$s and $T_2$ = 800 ns. Hyperfine interactions in $P^+$: four nitrogens with $a_N$ = 0.082 mT. Hyperfine interactions in $Q^-$: four deuterons with $a_D$ = 0.076 mT.

Although the major features of the magnetic interactions in the $[QFe^{2+}]^-$ complex are now resolved,[26-28] the g-tensor orientations in the lowest doublets are not known in any great detail.[53] Investigation of the observed *quantum beats* as a function of the detection field could provide this information. We are therefore analyzing the two-dimensional experiment, depicted in Figure 1b, in terms of an extended Hamiltonian, which accounts for high-spin $Fe^{2+}$ and its interaction with $Q^-$.[28] From the results we expect to assess the effect of $Fe^{2+}$ on the spin dynamics of the short-lived intermediates in the primary steps of bacterial photosynthesis.

Finally, quinone replacement could provide a means to vary the electron-transfer rate from the primary to the secondary rp.[14,15,56] Thus, electron spin polarization could be studied with primary rp lifetimes of 200 ps in native bacterial rcs to 10 ns in quinone replaced preparations.[15] In the latter case triplet admixture is expected to occur in the precursor pair, giving rise to significant phase and amplitude variations in the *quantum beat oscillations*.

## Conclusion

Using high time resolution transient EPR we have been able to detect *quantum beat oscillations* in the transverse magnetization of spin-correlated rps generated by pulsed laser excitation of photosynthetic bacterial rcs. Thorough investigation of these coherences allows a more detailed characterization of the short-lived intermediates of bacterial photosynthesis. It appears that *quantum beam oscillations* represent sensitive molecular probes for the study of the primary steps in natural photosynthesis.

**Acknowledgment.** Financial support by the U.S. Department of Energy, Office of Basic Energy Sciences, Division of Chemical Sciences (Contract W-31-109-ENG-38) and by the Deutsche Forschungsgemeinschaft is gratefully acknowledged. J.R.N. greatly acknowledges support from the Humboldt Foundation.

(56) Gunner, M. R.; Dutton, P. L. *J. Am. Chem. Soc.* **1989**, *111*, 3400–3412.